

## Hybrid DFT Study of the Mechanism of Quercetin 2,3-Dioxygenase

Per E. M. Siegbahn\*

Department of Physics, Stockholm Centre for Physics, Astronomy and Biotechnology (SCFAB),  
Stockholm University, S-106 91 Stockholm, Sweden

Received February 4, 2004

The mechanism of the copper-containing enzyme quercetin 2,3-dioxygenase has been studied using hybrid density functional theory. This enzyme cleaves the O-heterocycle of a flavonol using dioxygen and releases carbon monoxide. Two different pathways for the dioxygen attack on the copper complex have been investigated, and the one where the first attack is on copper is found to be the energetically preferred one. By using this pathway the problem of having to go through a spin-orbit-induced spin crossing is also avoided. The adduct has three unpaired spins and is ideally suited for forming a dioxygen bridging structure, which occurs in the next step. Rather than cleaving the O–O bond in the next step, another C–O bond between dioxygen and the substrate is first formed. Finally, the O–O bond is cleaved, and CO is released in one concerted transition state with a very low barrier. The results are in good agreement with experimental findings. The mechanism is compared to the ones for other similar enzymes studied recently by similar methods.

## I. Introduction

Dioxygenases are enzymes that catalyze the incorporation of both oxygens of dioxygen into their substrates. Their main biological importance relates to their ability to degrade aromatic compounds, but they also have other functions.<sup>1,2</sup> Quercetin 2,3-dioxygenase (2,3QD) is the only known member of this family which contains copper.<sup>3–5</sup> Most of the other ones contain non-heme iron, but dioxygenases containing manganese and magnesium are also known.<sup>6,7</sup> The substrate reaction catalyzed by 2,3QD is shown in Figure 1. The substrate quercetin is a 3,5,7,3',4'-pentahydroxy flavone. The O-heterocycle of the polyphenolic flavonol is cleaved, and carbon monoxide is released. The reaction is calculated to be exothermic by 88.9 kcal/mol. Apart from the different substrates, the reaction in the figure also differs from the non-heme iron intra- and extradiol dioxygenases by releasing carbon monoxide.<sup>8,9</sup>

The X-ray structure of quercetin 2,3-dioxygenase was first available without substrate at a resolution of 1.6 Å<sup>10</sup> but has also recently become available anaerobically complexed with the substrate quercetin to a resolution of 1.70 Å for *Aspergillus japonicus*.<sup>5,11,12</sup> The active site of the latter structure is shown in Figure 2. Before substrate binding, the Cu(II) metal ion is chiefly bound in a distorted tetrahedral geometry ligated by three histidines (His66, His68, and His112) and a water molecule. Upon anaerobically binding the substrate, the structure changes to a pentacoordinated square pyramidal geometry by replacement of the water and additional binding of a glutamate (Glu73) and the substrate. His66, His112, Glu73, and the O3 atom of the substrate form the equatorial base, and His68 is the apical ligand. One interesting feature of the structure is that the substrate O3 and Glu73 are at hydrogen bonding distance, indicating that the proton of the substrate might be positioned on the glutamate. Another interesting feature is that the substrate becomes bent at the C2 atom which is pyramidalized, indicating a possible radical site at this atom.

\* E-mail: ps@physto.se.

- (1) Hayaishi, O. In *Molecular Mechanisms of Oxygen Activation*; Hayaishi, O., Ed.; Academic: New York, 1974; pp 1–28.
- (2) Broderick, J. B. *Essays Biochem.* **1999**, *34*, 173–189.
- (3) Oka, T.; Simpson, F. J. *Biochem. Biophys. Res. Commun.* **1971**, *43*, 1–5.
- (4) Sharma, H. K.; Vaidyanathan, C. S. *Eur. J. Biochem.* **1975**, *56*, 163–171.
- (5) Steiner, R. A.; Kooter, I. M.; Dijkstra, B. W. *Biochemistry* **2002**, *41*, 7955–7962.
- (6) Boldt, Y. R.; Sadowski, M. J.; Ellis, L. B. M.; Que, L., Jr.; Wackett, L. P. *J. Bacteriol.* **1995**, *177*, 1225–1232.
- (7) Gibello, A.; Ferrer, E.; Martín, M.; Garrido-Pertierra, A. *Biochem. J.* **1994**, *301*, 145–150.

- (8) Que, L., Jr. *Chem. Rev.* **1996**, *96*, 2607–2624.
- (9) Solomon, E. I.; Brunold, T. C.; Davis, M. I.; Kemsley, J. N.; Lee, S.-K.; Lehnert, N.; Neese, F.; Skulan, A. J.; Yang, Y.-S.; Zhou, J. *Chem. Rev.* **2000**, *100*, 235–349.
- (10) Fusetti, F.; Schröter, K. H.; Steiner, R. A.; van Noort, P. I.; Pijning, T.; Rozeboom, H. J.; Kalk, K. H.; Egmond, M. R.; Dijkstra, B. W. *Structure* **2002**, *10*, 259–268.
- (11) Steiner, R. A.; Meyer-Klaucke, W.; Dijkstra, B. W. *Biochemistry* **2002**, *41*, 7963–7968.
- (12) Steiner, R. A.; Kalk, K. H.; Dijkstra, B. W. *Proc. Natl. Acad. Sci. U.S.A.* **2002**, *99*, 16625–16630.

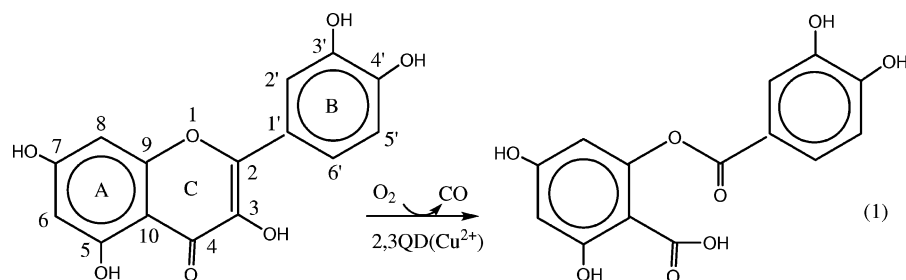


Figure 1. Reaction catalyzed by 2,3QD.

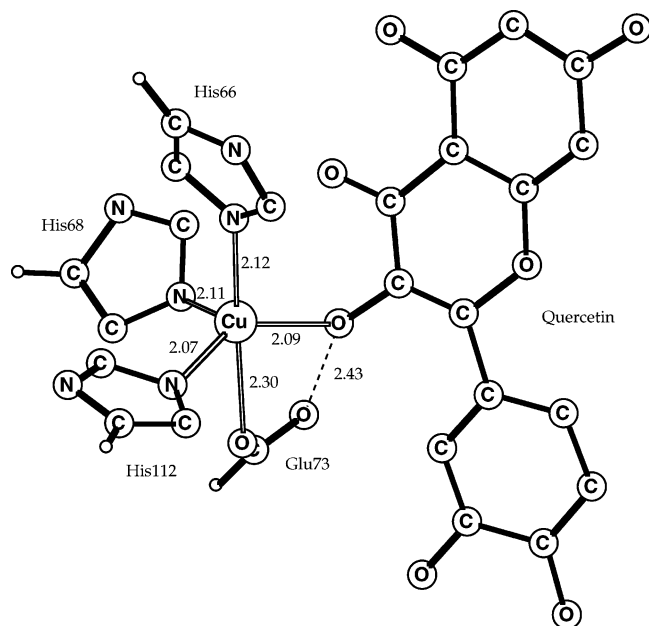


Figure 2. X-ray structure of the region around the Cu complex at the active site of quercetin 2,3-dioxygenase. The axial N–Cu–O angle is 105.0°, and the equatorial N–Cu–O angles are 90.1° and 140.9°.

On the basis of the X-ray structures, EPR investigations,<sup>13</sup> and biomimetic studies,<sup>14–17</sup> a possible mechanism was set up, see Figure 3, from here on termed the experimental mechanism.<sup>12</sup> The biomimetic studies were made on the substrate radical without the copper complex and showed that the same product was formed in the reaction with dioxygen as in the enzyme. The first step of the suggested mechanism is the substrate binding and was already partly described above. The substrate becomes bound by its O3 atom, and the proton is transferred to Glu73. The possible near degeneracy between the [Cu(II)–substrate] and [Cu(I)–substrate(rad)] states is implicated in the mechanism. In the next step, dioxygen attacks the complex. Two possibilities were discussed: one where O<sub>2</sub> directly attacks the substrate, shown in the figure, and one where it first attacks Cu(II) and then the substrate. The former pathway

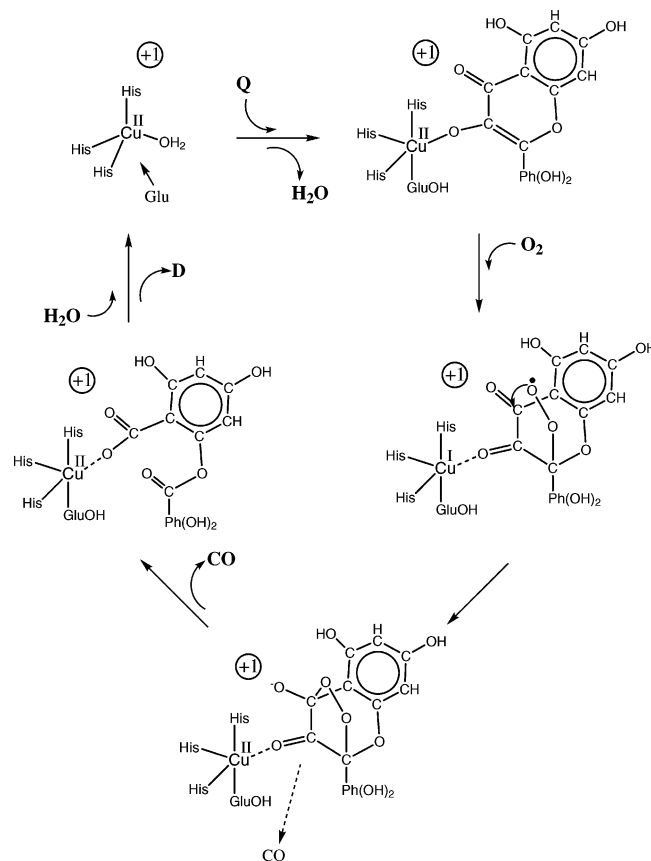


Figure 3. Reaction mechanism suggested by experiments.

was advocated mainly since the biomimetic studies showed that the substrate radical reaction gives the same reaction products, but also because O<sub>2</sub> normally does not bind to Cu(II), and because this pathway appears more geometrically feasible. In the third step dioxygen binds with both its oxygen atoms to the substrate. Finally, the O–O bond is cleaved, concertedly with cleavage of the C–C bonds and release of CO. The proposed mechanism suggests that the only difference between the biomimetic reaction and the one in the enzyme is the way in which the flavonoxyl radical is generated, where the enzyme uses the redox properties of Cu(II). The mechanism bears resemblance to the one suggested for intradiol Fe(III) catechol dioxygenases.<sup>18</sup> It should be added in this context that these enzymes are not evolutionary related, but their apparent mechanistic similari-

(13) Kooter, I. M.; Steiner, R. A.; Dijkstra, B. W.; van Noort, P. I.; Egmond, M. R.; Huber, M. *Eur. J. Biochem.* **2002**, *12*, 2971–2979.

(14) Speier, G. In *Dioxygen Activation and Homogeneous Catalytic Oxidation*; Simandi, L. I., Ed.; Elsevier Science: Amsterdam, 1991; pp 269–278.

(15) Balogh-Hergovich, E.; Kaizer, J.; Speier, G. *J. Mol. Catal.* **2000**, *159*, 215–224.

(16) Barhacs, L.; Kaizer, J.; Speier, G. *J. Mol. Catal.* **2001**, *172*, 117–125.

(17) Barhacs, L.; Kaizer, J.; Pap, J.; Speier, G. *Inorg. Chim. Acta* **2001**, *320*, 83–91.

(18) Que, L., Jr. In *Bioinorganic Catalysis*; Reedijk, J., Bouwman, E., Eds.; Dekker: New York, 1999; pp 269–321.

ties support the view that the copper site of 2,3QD has evolved from a preexisting, possibly iron-containing metal center.<sup>5</sup>

With high-accuracy X-ray structures available, the mechanism of 2,3QD is ideally suited for a study using quantum chemical models. In the present study, the plausible experimental mechanism in Figure 3 was used as a starting point, but other pathways were also investigated. As in previous studies,<sup>19–22</sup> hybrid DFT using the B3LYP functional has been used. Further information concerning the accuracy of the methods and models can be found in these reviews. The model used contains the metal complex including the first-shell ligands and substrate. No other residues were included since no additional groups have been implicated as being important for the mechanism. To stay reasonably close to the X-ray structures, one atom of each amino acid was frozen at its position in these structures. For the finally suggested mechanism, calculations were performed with and without the phenyl B-ring of the substrate. Comparisons will be made to previous and parallel studies on copper-containing enzymes such as tyrosinase,<sup>23,24</sup> catechol oxidase,<sup>25</sup> and amine oxidase<sup>26</sup> and to the iron-containing intradiol dioxygenase, which has a similar function as 2,3QD.

## II. Computational Details

The calculations were performed in three steps. For each structure considered, a full geometry optimization (with some atoms frozen from their positions in the X-ray structure) was performed using the hybrid density functional B3LYP method.<sup>27</sup> The present open-shell systems were treated with unrestricted DFT. In the first step, standard valence double- $\zeta$  basis sets were used for all light elements and for copper a nonrelativistic effective core potential (ECP).<sup>28</sup> The valence basis set used in connection with this ECP is essentially of double- $\zeta$  quality (the *lacvp* basis set). The same basis set was used also for the calculations of the Hessians for the smaller model of the substrate, without the phenyl B-ring, and the zero-point vibrational effects were taken from the results for this model. For the three most important transition states, Hessians were computed also for the larger model of the substrate to make sure that the geometries do not change between the models. Since some atoms were kept frozen, the computed thermal effects are not reliable, and these were therefore neglected. From previous experience, this should not qualitatively affect the general conclusions concerning the mechanism but could, of course, affect the energetics slightly. The only point where entropy effects are expected to be important is where dioxygen becomes bound, and this will be discussed in the text below. Another side effect of having some atomic positions frozen is that there tends to be a few small imaginary frequencies

in the optimized geometries. However, by graphical inspection of the normal modes, these frequencies are easily identified and not confused with transition states of interest.

Several aspects of freezing some atoms at their positions in the X-ray structure have been investigated and discussed elsewhere.<sup>22</sup> Two aspects will be mentioned here. First, it is very important to keep some atom frozen for the residues not anchored by the metal; otherwise they can start to move around unreasonably during the optimization. However, once the optimization has been completed, the constraints can often be released with only small energy changes, as found for thermolysin. Furthermore, for catechol oxidase the energetic effects of freezing coordinates from very different crystal structures were investigated.<sup>25</sup> Again, the effect was found to be small even though some positions frozen differed by more than one Angstrom. For the present system, all amino acids are anchored by copper; thus, the effects of freezing are expected to be small. Still, few tests were made by repeating the calculations without any constraints. For the reactant complex without dioxygen, the energy gain by releasing the constraints was found to be 6.1 kcal/mol. For the complex with dioxygen, the gain is 5.2 kcal/mol. The relative effect is thus 0.9 kcal/mol, which is almost within the roundoff errors of the calculations. The effect is quite similar for the TS of the dioxygen attack on the substrate. All these results are quite expected.

In the second step, the B3LYP energy was evaluated at the optimized geometries using a larger basis set, the *lacv3p\** basis set, which is of triple- $\zeta$  quality and uses a single set of polarization functions on each atom except the hydrogens.

In the third step, the surrounding protein was treated with a self-consistent reaction field method, using a Poisson–Boltzmann solver. The dielectric constant of the homogeneous dielectric medium was set equal to 4.0, in line with previous modelings of enzymes.<sup>30</sup> The probe radius was set to 2.50 Å to avoid artifacts sometimes appearing using a smaller probe radius.<sup>23</sup> No geometry optimizations including the dielectric continuum were made since the calculated dielectric effects were found to be quite small. A test was made of using a larger dielectric constant of 20.0 instead of 4.0 since site-directed mutagenesis appears to indicate a dielectric constant of this size.<sup>31</sup> For the step where the O<sub>2</sub> bridge was formed between copper and the substrate, the effect of increasing the dielectric constant to 20.0 was 0.2 kcal/mol on the computed barrier. This small effect is not surprising since the dielectric energy effects depend on the dielectric constant as  $(\epsilon - 1)/\epsilon$ . The energetic effect of changing the constant between 1.0 and 4.0 is therefore much larger than changing it between 4.0 and 20.0, and the total dielectric energy effect using 4.0 is by itself quite small for the present type of reactions. The calculations can thus in shorthand notation be written as B3LYP/*lacv3p\** energies including solvent contributions based on B3LYP/*lacvp* geometries. All calculations except of the Hessians were carried out using the Jaguar program.<sup>32</sup> The Hessians were calculated using Gaussian98.<sup>33</sup> The errors of using B3LYP for the present type of systems are usually smaller than 3 kcal/mol and seldom over 5 kcal/mol. Further information on the accuracy of B3LYP and the present type of chemical modeling of enzyme active sites containing transition metals can be found in several recent reviews.<sup>19–22</sup> To test the sensitivity of the B3LYP energies,

(19) Siegbahn, P. E. M.; Blomberg, M. R. A. *Annu. Rev. Phys. Chem.* **1999**, *50*, 221–249.

(20) Siegbahn, P. E. M.; Blomberg, M. R. A. *Chem. Rev.* **2000**, *100*, 421–437.

(21) Blomberg, M. R. A.; Siegbahn, P. E. M. *J. Phys. Chem. B* **2001**, *105*, 9375–9386.

(22) Siegbahn, P. E. M. *Q. Rev. Biophys.* **2003**, *36*, 91–145.

(23) Siegbahn, P. E. M. *J. Biol. Inorg. Chem.* **2003**, *8*, 567–576.

(24) Siegbahn, P. E. M.; Wirstam, M. *J. Am. Chem. Soc.* **2001**, *123*, 11819–11820.

(25) Siegbahn, P. E. M. *J. Biol. Inorg. Chem.*, in press.

(26) Prabhakar, R.; Siegbahn, P. E. M. *J. Am. Chem. Soc.*, in press.

(27) Becke, A. D. *Phys. Rev.* **1988**, *A38*, 3098. Becke, A. D. *J. Chem. Phys.* **1993**, *98*, 1372. Becke, A. D. *J. Chem. Phys.* **1993**, *98*, 5648.

(28) Hay, P. J.; Wadt, W. R. *J. Chem. Phys.* **1985**, *82*, 299.

(29) Pelmenschikov, V.; Blomberg, M. R. A.; Siegbahn, P. E. M. *J. Biol. Inorg. Chem.* **2002**, *7*, 284–298.

(30) Blomberg, M. R. A.; Siegbahn, P. E. M.; Babcock, G. T. *J. Am. Chem. Soc.* **1998**, *120*, 8812–8824.

(31) Garcia-Moreno, B.; Dwyer, J. J.; Gittis, A. G.; Lattman, E. E.; Spencer, D. S.; Stites, W. E. *Biophys. Chem.* **1997**, *64*, 211–224.

(32) *Jaguar 4.0*; Schrödinger, Inc.: Portland, OR, 1991–2000.

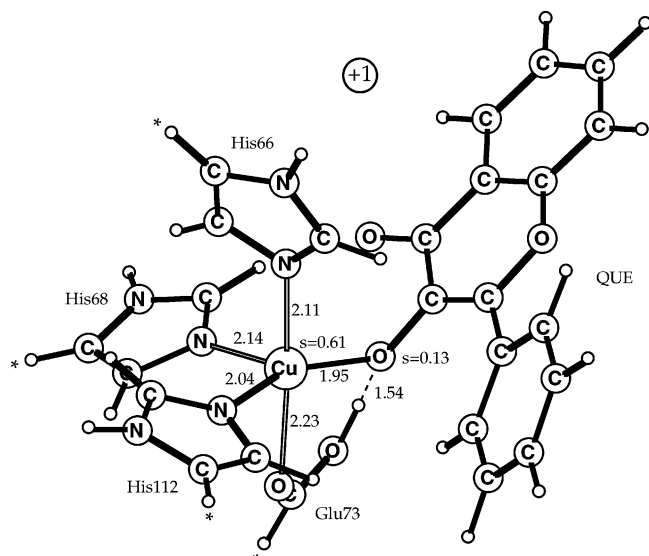


**Figure 4.** Optimized structure for the reactant of quercetin 2,3-dioxygenase. Distances are in Å, and spins larger than 0.10 are given. Atoms marked with an asterisk (\*) were frozen from the X-ray structure. The axial N–Cu–O angle is 101.4°, and the equatorial N–Cu–O angles are 100.6° and 154.5°.

the amount of exchange was reduced from 20% to 15% in single-point calculations for the entire mechanism. The results do not change the conclusions drawn based on the B3LYP energetics but indicate a few points where corrections may be needed. The results are described below.

### III. Results and Discussion

The mechanism of quercetin 2,3-dioxygenase (2,3QD) was studied using the model shown in Figure 4, in the figures termed QUE to differ it from the actual quercetin substrate Q. For comparison, calculations were also done for the substrate without the phenyl B-ring. As seen in the figure, the quercetin substrate was modeled with hydrogens rather than hydroxyl groups at the 5, 7, 3', and 4' positions. In the enzyme the hydroxyl groups of the substrate are not bound to the peptide but only to solvent waters, which means that the substrate should be comparably flexible at these points. The ligand histidines are modeled by imidazoles and the glutamate by a formate, as usual. This type of modeling has been demonstrated to work excellently for the energetics of enzyme mechanisms previously.<sup>21,22,34</sup> To further keep the optimized structures reasonably close to the experimental ones, one atom of each amino acid was frozen at its position in the X-ray structure, see the figure.

Two tests of the effects of leaving out the hydroxyl groups at the 5, 7, 3', and 4' positions have been made. First, the energy for reaction 1 was calculated with and without these hydroxyls, and the result changed by only 1.0 kcal/mol out of a total of 90 kcal/mol. Second, the binding of O<sub>2</sub> to the quercetin radical (discussed at the end of this section) was computed with and without the hydroxyls, and the difference was found to be only 0.3 kcal/mol. This error should be viewed in the context of error bars of 3–5 kcal/mol already expected for the present type of studies.

**a. Binding of O<sub>2</sub>.** The optimized structure in Figure 4 is reasonably close to the experimental one in Figure 2. The distances to the three histidines are around 2.10 Å, and the Cu–O distance to the glutamate is 2.20 Å compared to 2.30 Å in the X-ray structure. As indicated by the rather short Cu–O3 distance in the X-ray structure, the O3 proton prefers to stay at the Glu73 carboxylate. It will stay there until the end of the reactions, when it will be donated back to the substrate. The reason the Cu–O distance is somewhat shorter in the optimized than in the X-ray structure is that the hydrogen bond to O3 of the substrate is slightly too strong, thereby making the carboxylate more negative. This is a common finding using a small DZ-type basis set for the geometry optimization, and the distance would most likely improve with a larger basis set. However, there are by now numerous examples showing that these types of minor errors do not influence the energetics significantly and therefore not the conclusions concerning mechanisms either,<sup>22,34</sup> and the more time-consuming optimizations using a larger basis were therefore not done. The spin distribution, also shown in the figure, is characteristic of Cu(II). The spin population on copper is about 0.6, and the rest of the spin is spread out on the atoms ligating copper, the three nitrogens and the oxygen with slightly more spin on the O3 oxygen. The total charge of the model is +1. The details of the charge distribution are not given since these are seldom important for the mechanism. One reason for this is that the charges do not change much. For example, the charge on copper in all the optimized structures discussed in this paper are all in the narrow range +0.67 to +0.74.

One of the most interesting questions in connection with the mechanism of 2,3QD is where dioxygen binds. There are essentially two possibilities, either directly on the substrate or in the empty position on copper. These two pathways were considered in the experimental mechanism<sup>12</sup> in Figure 3, and the former one was chosen as more probable mainly on the basis of the biomimetic experiments using substrate radicals.<sup>14–17</sup> It is clear that the electronic ground-state [Cu(II)–substrate] configuration will bind dioxygen quite poorly, and other low-lying excited states are therefore of interest. Cu(III) is unlikely to be involved since this state has been found to be quite high in energy.<sup>24</sup> The most interesting low-lying excited state is instead [Cu(I)–substrate(radical)]. The same conclusion was reached in the experimental study.<sup>5</sup> However, when this state is considered, one still has the two possibilities of binding dioxygen described above, since dioxygen is likely to bind well both to Cu(I) and to the substrate radical. With the present model,

(33) Frisch, M. J.; Trucks, G. W.; Schlegel, H. B.; Scuseria, G. E.; Robb, M. A.; Cheeseman, J. R.; Zakrzewski, V. G.; Montgomery, J. A., Jr.; Stratmann, R. E.; Burant, J. C.; Dapprich, S.; Millan, J. M.; Daniels, A. D.; Kudin, K. N.; Strain, M. C.; Farkas, O.; Tomasi, J.; Barone, V.; Cossi, M.; Cammi, R.; Mennucci, B.; Pomelli, C.; Adamo, C.; Clifford, S.; Ochterski, J.; Petersson, G. A.; Ayala, P. Y.; Cui, Q.; Morokuma, K.; Malick, D. K.; Rabuck, A. D.; Raghavachari, K.; Foresman, J. B.; Cioslowski, J.; Ortiz, J. V.; Stefanov, B. B.; Liu, G.; Liashenko, A.; Piskorz, P.; Komaromi, I.; Gomperts, R.; Martin, R. L.; Fox, D. J.; Keith, T.; Al-Laham, M. A.; Peng, C. Y.; Nanayakkara, A.; Gonzalez, C.; Challacombe, M.; Gill, P. M. W.; Johnson, B.; Chen, W.; Wong, M. W.; Andres, J. L.; Head-Gordon, M.; Replogle, E. S.; Pople, J. A. *Gaussian 98*; Gaussian Inc.: Pittsburgh, PA, 1998.

(34) Siegbahn, P. E. M. *J. Comput. Chem.* **2001**, *22*, 1634–1645.

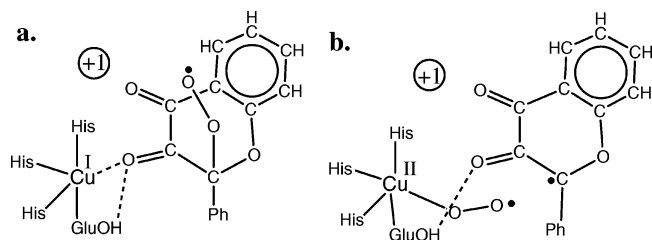


**Figure 5.** Possible binding modes of dioxygen (a) on the quercetin substrate and (b) on copper.

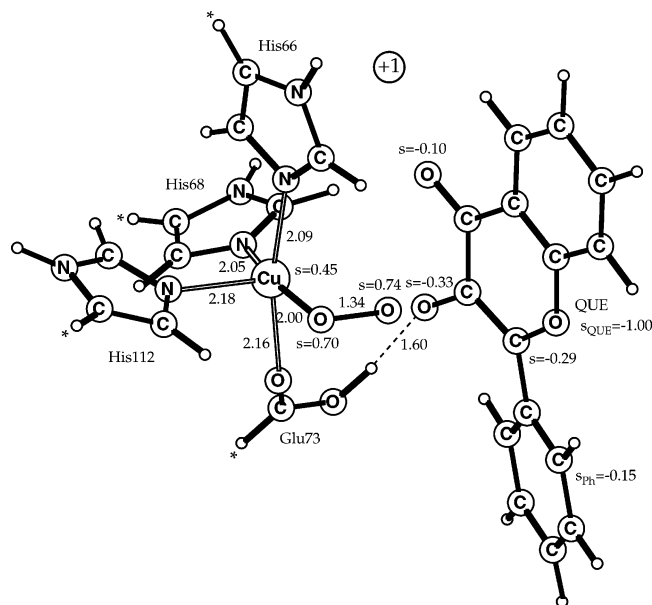


**Figure 6.** Optimized structure for the dioxygen adduct of quercetin 2,3-dioxygenase. Distances are given in Å, and spins larger than 0.10 are given. Atoms marked with an asterisk (\*) were frozen from the X-ray structure.

dioxygen is found to bind much better to copper than to the substrate by 14 kcal/mol. Still, the binding is found to be endothermic by 9.6 kcal/mol compared to the reactant and free dioxygen (the result with only 15% exchange is 8.3 kcal/mol). Apparently, there is a rather large cost involved in reaching the  $[\text{Cu(I)}\text{-substrate(radical)}]$  state. This energy cost is to a large extent due to the formation of the  $\text{C}=\text{O}$  double bond on the substrate, which forms a much weaker bond to copper than the previous  $\text{C}-\text{O}^-$  group does. The large endothermicity of 23.5 kcal/mol for the binding of dioxygen directly to the substrate is rather surprising but makes the conclusion to rule out that pathway quite safe even if there should be unexpectedly large errors in the calculations.

Since it is the state  $[\text{Cu(I)}\text{-substrate(radical)}]$  that will bind dioxygen, the excitation energy to reach this state will affect the binding energy. This is the case irrespective of where the binding occurs. In the optimized structure in Figure 6 one can see that there is one spin on the substrate when dioxygen binds to copper. It can be noted that this structure is the only one of the present structures where the expectation value of  $S^2$  is substantially different from the correct value of 0.75. The calculated value is 1.76, showing a strong mixture with the quartet state, as expected with the spin distribution given in the figure. However, this spin contamination does not have any effect on the energy. The quartet state was optimized giving an energy that differs by only

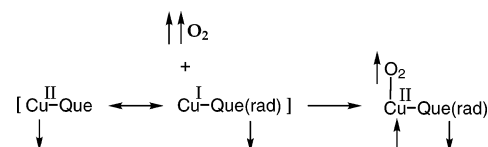


**Figure 7.** Spin distribution for the reaction between the copper complex and dioxygen.

0.2 kcal/mol. A simple way to modify the stability of the substrate radical is to replace the phenyl B-group by a hydrogen, which should have a destabilizing effect. When this is done the effect is as expected and dioxygen binding on copper becomes endothermic by 13.3 kcal/mol rather than 9.6 kcal/mol with the full substrate. The main difference in the spin distribution between the two substrates is at the C2 position. In the full substrate the spin population is  $-0.29$  on C2 and  $-0.15$  on the phenyl ring, while without the phenyl the spin on C2 is  $-0.40$ . The spin on copper is 0.45 for the large models and 0.44 in the small one, while the spin on dioxygen is 1.44 (1.43).

It is interesting to note that the above argument can be applied also on the non-heme iron intradiol dioxygenases. In that case a similar low-lying state has also been suggested to simplify dioxygen binding. The reactant is an  $\text{Fe(III)}\text{-catechol}$  complex, and the corresponding excited state will then be  $[\text{Fe(II)}\text{-catechol(radical)}]$ .<sup>8,18</sup> Like in the case of 2,3-QD, the presence of this low-lying excited state has been used to suggest that dioxygen might attack the substrate directly. However, also in that case dioxygen attack on the metal is found to be preferred. For an earlier study of dioxygen attack in intradiol dioxygenase, see also ref 35.

A consequence of the formation of the substrate radical at C2 is that the single  $\text{C}-\text{O}$  bond at C3 will become a double bond. This, in turn, leads to a loss of binding between  $\text{Cu(II)}$  and the substrate. The  $\text{Cu}-\text{O3}$  distance becomes as large as 3.78 Å. This is partly due to a very flat potential surface. Decreasing the  $\text{Cu}-\text{O3}$  distance to 2.20 Å only costs 2.6 kcal/mol, which is thus an upper bound for the effect of protein strain on this step. However, from previous experience the effect of protein strain is likely to be even smaller.

Whenever dioxygen is involved in reactions with closed shell substrates there is a spin-transition problem since dioxygen is a triplet while the reactant and product are singlets. Without any metal present the only solution is to form high-energy biradical states or to involve spin-orbit effects. By the formation of the dioxygen structure in Figure 6 the spin-transition problem is solved through the formation of a low-energy complex with three unpaired spins, see Figure 7. Dioxygen reacts with the low-lying state of the reactant, and one of the up-spins is simply delocalized from dioxygen to copper, keeping the down-spin on the substrate. From this point onward, the spins are decoupled and no further spin-forbidden processes are required. It should be noted that copper is particularly well suited for this process. For example, a high-spin iron would have to be transformed to one with lower spin in the same process, which would cost more energy.

(35) Funabiki, T.; Yamazaki, T. *J. Mol. Catal.* **1999**, *150*, 37–47.

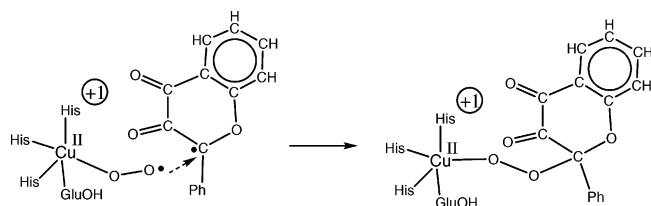


**Figure 8.** Second step of the suggested mechanism for 2,3QD.

Thus far, the expected entropy loss when dioxygen binds has not been considered. If the harmonic approximation is used and if the reactant and dioxygen are treated in two separate calculations, an entropy loss larger than 10 kcal/mol is obtained, which would lead to a too high barrier for the next step. The most careful treatment of dioxygen binding done so far is the one on hemerythrin using QM-MM methods to treat the entire enzyme.<sup>36</sup> An interesting effect found in that study is that van der Waals effects from the enzyme go in the opposite direction to the entropy loss and therefore cancel these to a large extent. Furthermore, reducing the exact exchange in B3LYP increases the dioxygen binding somewhat, see above. These two considerations together indicate that the best estimate for the binding of dioxygen that can be made at this stage is obtained if about 5 kcal/mol is added to the computed enthalpy of binding. Even if this estimate deserves further studies, it is concluded here that the most interesting conclusions of the present study will be unaffected by the precise size of these effects.

**b. Peroxide Bridge Formation.** In the next step, dioxygen should attack the substrate radical. This step is already well prepared with a spin on dioxygen of 1.44 and on the substrate of  $-1.00$ . The situation is quite similar for the non-heme extradiol dioxygenase, where the binding of dioxygen on iron leads to a peroxy radical and a radical on the deprotonated catechol substrate with opposite spin. The structure of the active complex in the biogenesis of the TPQ cofactor in copper-containing amine oxidase is even more similar.<sup>26</sup> The formation of the bridging peroxide is therefore expected to be quite simple. Indeed, the barrier counted from the dioxygen adduct is only 1.1 kcal/mol, which is 10.7 kcal/mol higher than the starting reactant and dioxygen (the barrier using only 15 exact exchange is 7.4 kcal/mol). One reason the barrier is so low is that the reactant dioxygen complex and the substrate radical are easily lined up for bridge formation since the direct bonding between the substrate and Cu(II) has been lost, see above. The optimized transition state is shown in Figure 9. The barrier can be compared to the ones in extradiol dioxygenase of 3.3 kcal/mol, in amine oxidase of 8.4 kcal/mol, and in tyrosinase of 12.3 kcal/mol. The reason the barrier is so much higher for tyrosinase is that the substrate radical state is not the ground state for the peroxy complex.

The main structural parameters of the transition state in Figure 9 are the O–C2 distance of 2.09 Å, the O–O distance of 1.37 Å, and the Cu–O distance of 1.98 Å. The corresponding distances for tyrosinase are 1.82, 1.49, and 2.04 Å

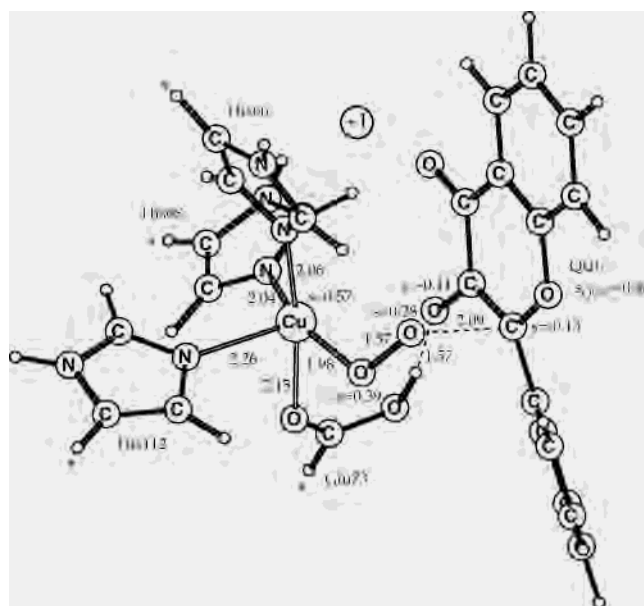


**Figure 9.** Optimized transition-state structure for the first C–O bond formation in 2,3-quercetin dioxygenase. Distances are given in Å, and spins larger than 0.10 are given. Atoms marked with an asterisk (\*) were frozen from the X-ray structure.

and for biogenesis in copper amine oxidase 2.10, 1.40, and 2.00 Å. At the transition state the spin on the quercetin has decreased from 1.00 to 0.40. Nearly all spin on the phenyl B-ring is gone. The hydrogen bond between O3 and Glu73 is almost unaffected by the bridge formation process. The Cu–O3 distance at the TS is 2.69 Å. As for the reactant of this step, see above, the cost of decreasing this bond to 2.20 Å is rather small, in this case 2.5 kcal/mol. This value should be an upper bound to the effect of protein strain. It is interesting to note that fixing the Cu–O3 distance at 2.20 Å affects the barrier for O<sub>2</sub> bridge formation by only 0.1 kcal/mol, counted from the peroxide adduct. The imaginary frequency at the TS is 219 cm<sup>-1</sup>. After passing the transition state the key bonds continue to change and the bridge formation becomes exothermic by 6.2 kcal/mol, counted from the dioxygen adduct (with 15% exact exchange the exothermicity becomes 8.0 kcal/mol). The spin on copper increases slightly to 0.63 from 0.57, and the spin on the substrate disappears entirely. No other spins are changed. For the smaller substrate without the phenyl B-ring, only a very small barrier of less than 1 kcal/mol was found, and the reaction was found to be exothermic by as much as 18.3 kcal/mol. One reason for this is that the spin is better localized on C2 in the small substrate. On the other hand, preparation of the dioxygen adduct is more costly in that case. Overall, the higher stability of the product complex is due to less repulsion between dioxygen and hydrogen than between dioxygen and phenyl.

**c. Third Step of the Catalytic Cycle.** At some stage the O–O bond in dioxygen must be cleaved. For copper amine oxidase, iron intradiol dioxygenase, and tyrosinase, the bridging dioxygen position is the point from which this bond cleavage occurs, see Figure 10. In amine oxidase the two electrons required for the cleavage come from the substrate; in intradiol dioxygenase, the two electrons are available from

(36) Wirstam, M.; Lippard, S. J.; Friesner, R. A. *J. Am. Chem. Soc.* **2003**, *125*, 3980–3987.

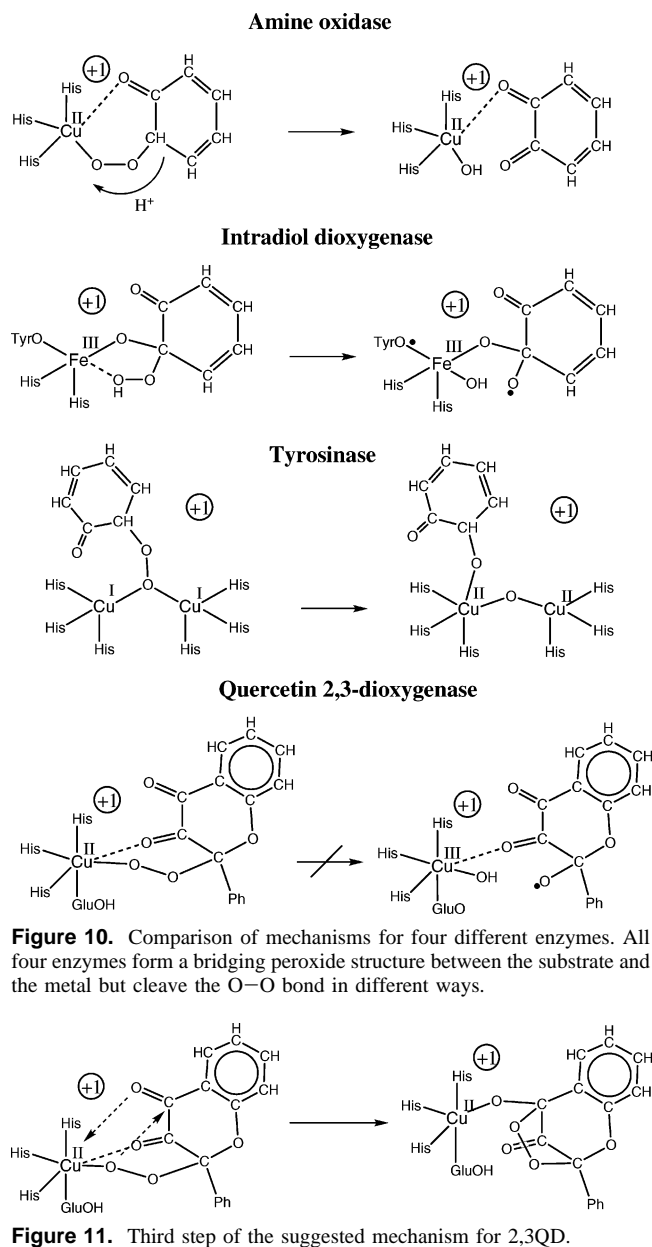


**Figure 10.** Comparison of mechanisms for four different enzymes. All four enzymes form a bridging peroxide structure between the substrate and the metal but cleave the O–O bond in different ways.

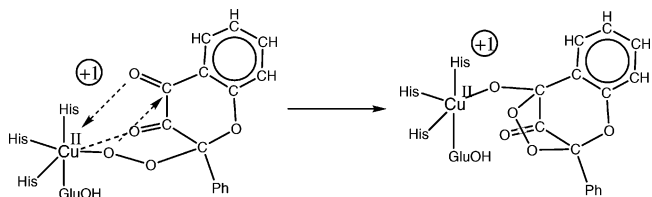


**Figure 11.** Third step of the suggested mechanism for 2,3QD.

iron + tyrosinate and the substrate; in tyrosinase, the two electrons can be obtained from the Cu(I) centers. However, the O–O cleavage is not energetically possible for 2,3QD at this point since two electrons are not easily available. A cleavage would lead to Cu(III) and a substrate radical. For 2,3QD, a second C–O bond between dioxygen and the substrate therefore first has to form before the O–O cleavage can occur, see Figure 11. The optimized transition state for this C–O bond formation, which occurs to C4 of the substrate, is shown in Figure 12. The critical C4–O distance is 1.93 Å, somewhat shorter than the 2.09 Å for the previous TS. The imaginary frequency is 136 cm<sup>-1</sup>. The barrier counted from the peroxide bridge minimum is only 7.1 kcal/mol (with 15% exact exchange it is 6.5 kcal/mol). No significant spin changes occur in this step. The reaction is endothermic by 4.5 kcal/mol. However, at the completion of the step a change of hydrogen bonding occurs which leads to a lowering of the energy by 2.8 kcal/mol. The Glu73

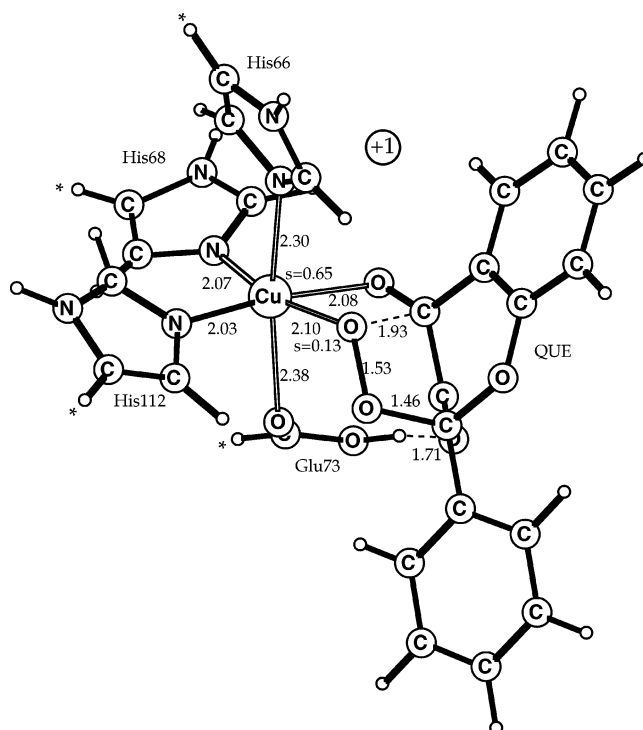


**Figure 12.** Optimized transition-state structure for the second C–O bond formation in quercetin 2,3-dioxygenase. Distances are given in Å, and spins larger than 0.10 are given. Atoms marked with an asterisk (\*) were frozen from the X-ray structure.

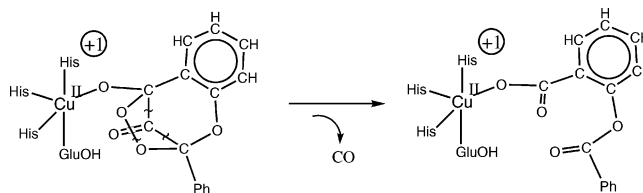


**Figure 13.** Fourth step of the suggested mechanism for 2,3QD.

hydrogen bond moves from O3 to O4. If this change is included in this step, it becomes endothermic by only 1.7 kcal/mol (with 15% exact exchange it is 1.9 kcal/mol). It should be noted that this change of hydrogen bonding is needed at some stage in the reaction sequence, since the proton on the glutamate should eventually end up on O4 while C3–O3 should become a carbon monoxide molecule. The small substrate model behaves similarly. The barrier is 12.7 kcal/mol, and the step is endothermic by 6.2 kcal/mol. Both these energies differ from the large model by about 5 kcal/mol, reflecting the high stability of the peroxide reactant for the small model.

**d. O–O Bond Cleavage.** The next reaction step is quite complicated with a simultaneous cleavage of the O–O bond and two C–C bonds, see Figure 13. The optimized transition state is shown in Figure 14. To find a sufficiently good starting geometry for this optimization, a pointwise search was made. There are actually as many as five critical bond distances for which the optimized values are 1.99 (O–O), 1.64 (C2–C3), 1.68 (C3–C4), 1.33 (C2–O), and 1.37 Å (C4–O). The two latter values are between the ones for the reactant of about 1.50 Å and the ones for the product of about 1.25 Å and are of key importance for finding the TS.

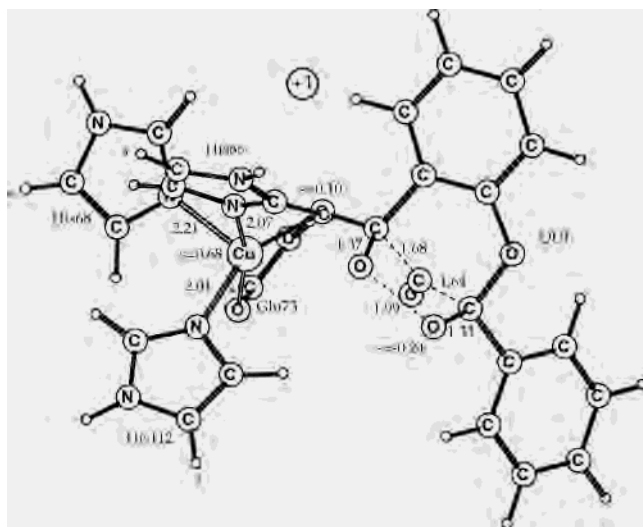


**Figure 14.** Optimized transition-state structure for O–O bond cleavage in quercetin 2,3-dioxygenase. Distances are given in Å, and spins larger than 0.10 are given. Atoms marked with an asterisk (\*) were frozen from the X-ray structure.

In the first attempt to find the TS (using the model without the phenyl B-ring) not enough attention was paid in the pointwise search to find good starting values for these C–O distances and the geometry optimization instead led toward a structure about 10 kcal/mol higher than the reactant. At that point the O–O bond is completely broken with an O–O distance of 2.4 Å. The electronic structure in this region is that of a substrate biradical with antiparallel spins on the oxygens. Since the antiparallel spins are so far from each other, the quartet state with parallel spins is quite similar in energy, only 0.5 kcal/mol lower. For the actual TS in Figure 14 the barrier is only 0.2 kcal/mol. Without dielectric effects (–0.2 kcal/mol) and zero-point energies (–2.4 kcal/mol) the barrier is 2.8 kcal/mol (with 15% exact exchange it is 0.7 kcal/mol). A graphical display of the imaginary frequency of 387 cm<sup>-1</sup> very clearly shows the correct character of the TS. The presence of the biradical state is probably not important for the low energy of the transition state since the spins of the oxygens at the TS are quite small, see the figure. The only significant spin is the one on one of the oxygens with –0.24. For the model with the smaller substrate the barrier is also very small with only 0.5 kcal/mol. After passing the TS the energy goes down very much all the way to the formation of the anionic product. The computed exothermicity of this step is as high as 101.8 kcal/mol (with 15 exact exchange it is 98.6 kcal/mol). For the small substrate model it is 95.5 kcal/mol.

**e. Substrate Radical Reactions.** Finally, the biomimetic reaction between O<sub>2</sub> and the substrate radical,<sup>14–17</sup> without the presence of the copper complex, was also studied. This is obviously a much simpler reaction to treat and led to useful starting structures for the reaction of the full model. Surprisingly, very few studies have been reported on similar reactions previously. Of the few examples found for reactions with triplet dioxygen, there is one with the ethyl radical<sup>37</sup>

(37) Andersen, A.; Carter, E. A. *J. Phys. Chem. A* **2002**, *106*, 9672–9685.

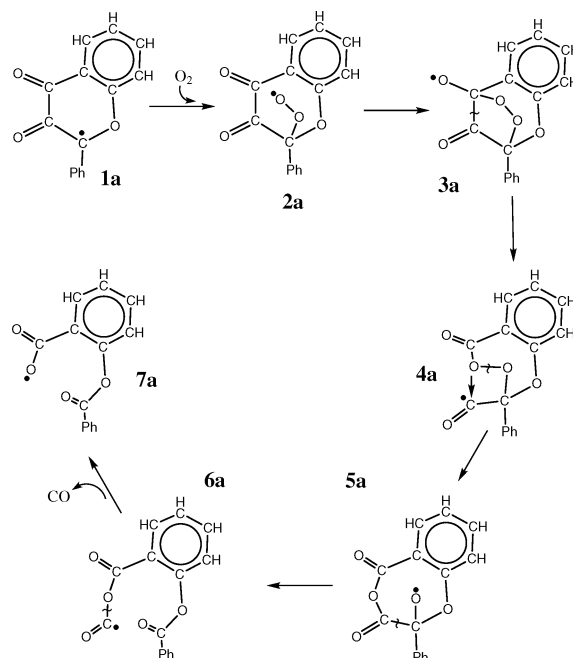


**Figure 15.** Suggested reaction sequence between dioxygen and the quercetin radical.

and one with alkoxy radicals.<sup>38</sup> However, even though the radical reaction has significant similarities to the enzyme reaction and led to the same products, there are also some notable differences. Once the substrate has formed the two bridging bonds to the oxygens, the enzyme reaction is nearly over. The only step remaining is the O–O bond cleavage, which goes over a small barrier and leads almost all the way to the product. In contrast, the radical reaction is found to go through several steps to form the product after the bridging dioxygen structure has been formed, see Figure 15. The energetics (without entropy contributions) are shown in Figure 16. These reactions were studied without the phenyl B-ring.

The rate-limiting step of the radical sequence in Figure 15 is the formation of the second, bridging, C–O bond (**3a**). This step has a calculated barrier of 21.0 kcal/mol, which might become somewhat lower with the addition of the phenyl B-ring. This step is substantially endothermic by 18.2 kcal/mol. It is interesting to note that the reaction between O<sub>2</sub> and the nonradical quercetin substrate to form a bridging singlet peroxide species is endothermic by only 2.1 kcal/mol but obviously has a much higher barrier and involves a spin transition. The cleavage of the C–C bond in **3a** in the next step of the radical reactions only has a barrier for the small basis set but none with the larger basis. This step is exothermic by 17.4 kcal/mol. With the large basis set, the picture of these two steps is therefore that of one step with a nonconcerted formation of the second C–O bond and a cleavage of the C–C bond. This single step has a barrier of 21.0 kcal/mol and an endothermicity of 0.8 kcal/mol. The subsequent O–O bond cleavage in **4a** has a small barrier of 2.1 kcal/mol and is strongly exothermic by 60.6 kcal/mol. The next step of C–C bond cleavage in **5a** also has a low

(38) Setokuchi, O.; Sato, M. *J. Phys. Chem. A* **2002**, *106*, 8124–8132.



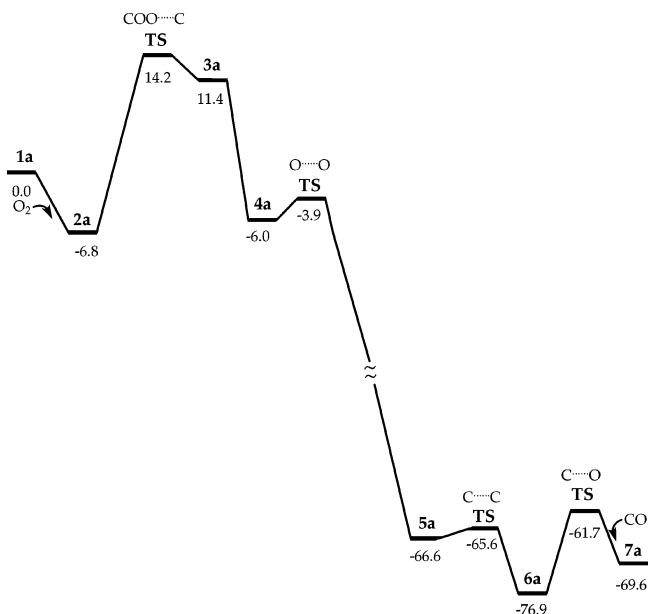


**Figure 16.** Energetics for the suggested reaction sequence between dioxygen and the quercetin radical. The numbers for the structures are those from Figure 15.

barrier of 1.0 kcal/mol and is exothermic by 10.3 kcal/mol. The final step of CO release from **6a** goes over a barrier of 15.2 kcal/mol and is endothermic by 7.3 kcal/mol. This step is obviously strongly modified by entropy, which may even make it exergonic.

In a comparison of the mechanisms of 2,3QD on one hand and the non-heme iron intra- and extra-diol dioxygenases on the other, it is interesting to compare the properties of the substrates themselves. As described above, for 2,3QD, dioxygen binds with both its oxygens to quercetin at one stage of the mechanism. This pathway has been found to be too high in energy for the catechol dioxygenases. The origin of this difference is found in the binding energy between  $O_2$  and the (nonradical) substrates. For quercetin, the binding of  $O_2$  to form a singlet bridging dioxygen species as in Figure 11 is endothermic by only 2.1 kcal/mol. For catechol, the corresponding binding is endothermic by as much as 20.1 kcal/mol. The reason is clearly the higher cost in breaking up the aromaticity of the catechol.

#### IV. Conclusions

The suggested mechanism for 2,3QD, described above, is summarized in Figure 17 and the energetics in Figure 18. In the starting structure **1**, the quercetin substrate has lost a proton to Glu73 and become ionically bound to copper. In the next step, dioxygen attacks the complex. The present calculations give a very clear preference for an attack on copper rather than on the substrate. To make this binding possible, a low-lying excited state is involved. This is the [Cu(I)–substrate(radical)] state, which means that the product of the oxygen attack will remain a Cu(II) complex but with a substrate radical. By involving this low-lying excited state there is furthermore no need for any spin–orbit-induced spin transition since dioxygen can simply delocalize one of its spins on copper. Copper is unusually well adapted for this

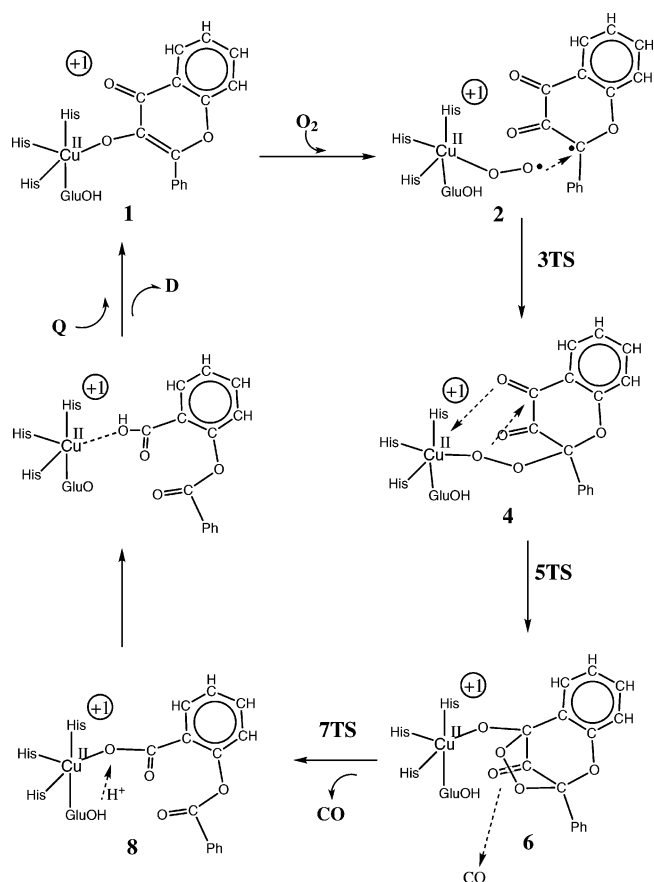


**Figure 17.** Suggested catalytic cycle for 2,3QD.

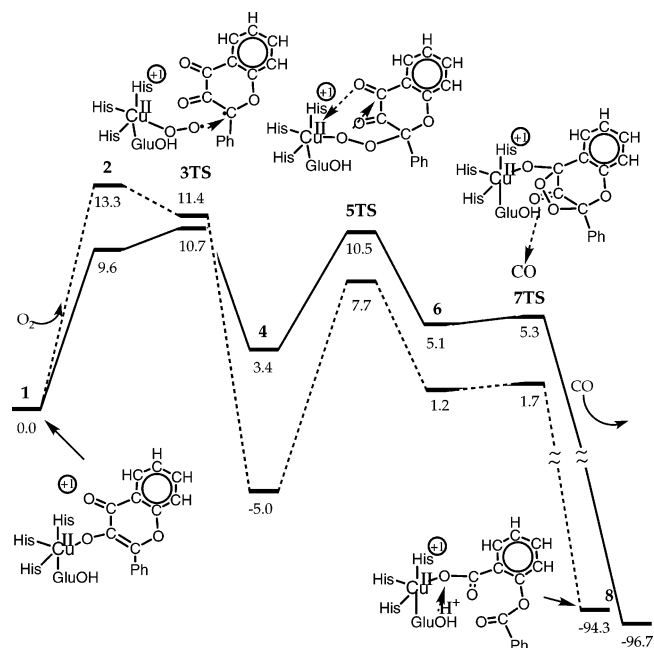


**Figure 18.** Energetics for the suggested catalytic cycle for 2,3QD. The numbers for the structures are those from Figure 17. The dashed line corresponds to the results where the phenyl B-ring has been removed.

process since no recoupling of the d electrons is needed, which would be the case for a high-spin iron complex, for example. The binding of dioxygen is found to be endothermic by as much as 9.6 kcal/mol. Entropy effects, not included in Figure 18, are expected to make the endergonicity even

higher. As discussed above, the entropy effects are very difficult to calculate but can be estimated to be somewhere in the range 0–5 kcal/mol. It is therefore likely that this first step of O<sub>2</sub> binding is rate limiting for the whole cycle.

Since the peroxy radical and the substrate have opposite spins, the dioxygen adduct structure **2** is perfectly set up for the next step of the suggested mechanism, which is the formation of the first C–O bond. This step goes over a very small barrier of 1.1 kcal/mol and is exothermic by 6.2 kcal/mol. It is interesting to compare these two steps with the ones for a substrate without the phenyl group, which should have a less stable radical state. In line with this, the formation of the dioxygen adduct is 3.7 kcal/mol less stable than for the full substrate. However, the barrier for formation of the first C–O bond is smaller and the exothermicity larger without the phenyl ring. The stronger localization of the spin and the less repulsion of oxygen to hydrogen than to phenyl explain these results.

For many enzymes the next step after the bridging peroxide **4** has been formed would be the cleavage of the O–O bond. However, this pathway is not the preferred one for 2,3QD since Cu(III) is too high in energy. Instead, a second C–O bond between the peroxide and substrate is formed. The barrier for this step is also quite low with 7.1 kcal/mol, and the reaction is only slightly endothermic by 1.7 kcal/mol. This endothermicity also involves a change of hydrogen bonding to Glu73, which is energetically favorable and

advantageous for reaching the final product. It is interesting to note that this type of pathway, with formation of a second C–O bond, is quite unfavorable for catechol dioxygenases since the cost of breaking the aromaticity of the catechol is too high.

The final step of the mechanism is the most complicated one involving the simultaneous cleavage of the O–O bond and two C–O bonds. The transition state was also quite difficult to find involving five important reaction coordinates. Still, the barrier obtained is very low with only 0.2 kcal/mol when solvent and large basis sets effects are added. The reason for the low barrier is that the reaction is very strongly driven by an extremely large exothermicity of over 100 kcal/mol. In the final step, the proton stored on Glu73 goes back to the substrate, which then leaves.

As a comparison, the biomimetic reaction between dioxygen and the quercetin radical was also studied. Even though this reaction leads to the same product as for the enzyme, the mechanisms are rather different. In the radical case, the formation of the second, bridging C–O bond is the rate-limiting step, followed by the step where CO is released.

**Supporting Information Available:** Cartesian coordinates, energies, and  $S^2$  expectation values for the structures shown in the figures. This material is available free of charge via the Internet at <http://pubs.acs.org>.

IC0498541